Full paper / mémoire

New bulk weak ferromagnet in ferrimagnetic chains of molecular material based on DTDH–TTP and paramagnetic thiocyanato complex anion: (DTDH–TTP)[Cr(isoq)₂(NCS)₄]

Fatima Setifi [a], Lahcène Ouahab [a,*], Stéphane Golhen [a], Akira Miyazaki [b],
Toshiaki Enoki [b], Jun-ichi Yamada [c]

[a] *LCSIM, UMR 6511 CNRS, université de Rennes–1, Institut de chimie de Rennes, 35042 Rennes cedex, France*
[b] *Department of Chemistry, Graduate School of Science and Engineering, Tokyo Institute of Technology,*
O-okayama, Meguro-ku, Tokyo 152–8551, Japan
[c] *Department of Material Science, Graduate School of Science, Himeji Institute of Technology,*
3–2–1 Kouto, Kamigori-cho Ako-gun, Hyogo 678–1297, Japan

Abstract

The preparation, X-ray crystal structure and magnetic properties of a new charge transfer salt, (DTDH–TTP)Cr(isoq)₂ (NCS)₄, DTDH–TTP = 2-(1′,3′-dithiol-2′-ylidene)-5-(1″,3″-dithiolan-2″-ylidene)-1,3,4,6-tetrathiapentalene, isoq = isoquinoline) are reported. Crystal data: monoclinic, space group $C2/c$ (#15), $a = 16.0836(5)$, $b = 19.2488(6)$, $c = 12.6829(6)$ Å, $\beta = 95.669(1)$, $V = 3906.5(2)$ Å³, $Z = 4$, $R = 0.0515$ for 2899 reflections with $I > 2\ \sigma(I)$. The crystal structure consists of mixed organic and inorganic layers in the ac-plane, each layer being formed by mixed columns of DTDH–TTP•⁺ radical cations and paramagnetic metal complex anions. Short intermolecular atomic contacts between donor and anion are observed in the column in the c direction. Ferrimagnetic interactions are observed between the non-equivalent donor and anion spins. This material exhibits bulk canted weak ferromagnetism below $T_C = 8.7$ K. *To cite this article: F. Setifi et al., C. R. Chimie 6 (2003).*

Résumé

Des efforts considérables sont actuellement concentrés sur les études de matériaux moléculaires polyfonctionnels qui présentent une coexistence ou, mieux encore, une synergie entre conductivité électrique et magnétisme. Plusieurs stratégies sont utilisées pour réaliser ce type de composés : (*i*) la synthèse de complexes de coordination dans lesquels le réseau paramagnétique et le réseau conducteur sont liés de manière covalente, comme par exemple [M(hfac)₂](TTF–py)₂ (M = Cu^II, Mn^II, hfac = hexafluoroacetylacetonate; TTF-py = 4-(2-tétrathiafulvalenylethenyl)pyridine) ; (*ii*) l'utilisation de donneurs fonctionnalisés et d'anions adéquats pouvant donner des interactions de type –CN···X– ; (*iii*) l'assemblage de donneurs organiques avec des complexes d'ion de transition à ligands π pouvant donner des interactions S···S et/ou –CN···X–. Ainsi, de nombreux composés présentant un ordre ferri- ou ferromagnétique ont été obtenus selon cette dernière stratégie. Nous présentons dans cet article la préparation, la structure cristallographique et les propriétés magnétiques d'un nouvel aimant moléculaire (DTDH–

* Corresponding author.
E-mail address: ouahab@univ-rennes1.fr (L. Ouahab).

TTP)Cr(isoq)$_2$(NCS)$_4$, DTDH–TTP = 2-(1',3'-dithiol-2'-ylidene) -5-(1″,3″-dithiolan-2″-ylidene)-1,3,4,6-tétrathiapentalene, isoq = isoquinoline). Données cristallographiques : monoclinique, groupe d'espace $C2/c$ (#15), $a = 16.0836(5)$, $b = 19.2448(6)$, $c = 12.6829(6)$Å, $\beta = 95.669(1)$, $V = 3906.5(2)$Å^3, $Z = 4$, $R = 0.0515$ pour 2899 réflexions avec $I > 2\ \sigma(I)$. La structure cristalline contient des couches mixtes organiques–inorganiques en zig-zag. Chaque couche est formée de colonnes mixtes de radicaux cations DTDH–TTP $^{\bullet+}$ et de complexes paramagnétiques. Des contacts intermoléculaires courts existent entre les radicaux organiques et les anions inorganiques dans la direction c. Des interactions ferrimagnétiques sont observées entre les spins non équivalents des radicaux cations organiques et des anions. Ce composé présente un ordre ferromagnétique faible incliné en dessous de $T_C = 8.7$ K. ***Pour citer cet article : F. Setifi et al., C. R. Chimie 6 (2003).***

1. Introduction

One of the current challenges in molecular science is to prepare new compounds with combinations of two physical properties as for example magnetic interactions and electrical conductivity [1–9]. The strategy used up to now consists in assembling together conducting organic sublattice and paramagnetic inorganic sublattice in salts made of organic radical ions derived from TTF, tetrathiafulvalene and paramagnetic inorganic counter-ions. This yields in general materials with weak interactions (when they exist) between the two systems. In order to establish such interactions, we are investigating several ideas: (*i*) the synthesis of new materials where the conducting and magnetic systems are covalently linked through π-conjugated bridge, such as [M(hfac)$_2$](TTF–py)$_2$ (M = Cu^{II}, Mn^{II}, hfac = hexafluoroacetylacetonate; TTF–py = 4-(2-tetrathiafulvalenylethenyl)pyridine) [9]; (*ii*) the assemblies of functionalized organic donors bearing –OH or halogen (–X) functions and paramagnetic cyano complex anions, with the aim to mediate magnetic interaction through hydrogen bonding or –CN···X–interactions [5]; (*iii*) the assemblies of organic donors with cyano or thiocyanato paramagnetic transition metal complexes involving π ligands (see scheme). This might yield short S···S and/or –CN···X– contacts between the donors and the anions and also π–π overlap between the ligand of the anion and the π system of the donor molecule. Hence, numerous salts were obtained with this strategy and showed bulk ferrimagnetism and weak bulk ferromagnetism [8]. Recently developed

tetrathiapentalene(TTP)-derived donors have high tendencies of producing metallic salts down to low temperatures, and also have potential to give molecular magnets as evidenced by an antiferromagnetic transition in β-(BDA–TTP)$_2$FeCl$_4$ (BDA–TTP = 2,5-bis (1',3'-dithian-2'-ylidene)-1,3,4,6-tetrathiapentalene) [10]. We have therefore focused on this series of donors and developed a molecular magnet (BDH–TTP)[Cr(isoq)$_2$(NCS)$_4$], where BDH–TTP and isoq are 2,5-bis(1',3'-dithiolan-2'-ylidene)-1,3,4,6-tetrathiapentalene and isoquinoline, respectively [11]. This salt shows a weak ferromagnetism with the transition temperature $T_C = 7.6$ K, whose magnetic structure is characterized from single-crystal magnetic measurements as a spin-canted weak ferromagnetism derived from the single-ion anisotropy of the anions. Among the series of TTP-derived donors, DTDH–TTP (2-(1,3-dithiolan-2-ylidene)-5-(1,3-dithiol-2-ylidene)-1,3,4,6-tetrathiapentalene) is found to produce metallic salts down to low temperatures depending on the counter-anions [12]. As this molecule has a C=C double bond at one of the molecular ends and the π-electron system is more delocalised than BDH–TTP, the on-site Coulomb repulsion on the donor is reduced and the intermolecular exchange interaction is expected to be increased. In the same time, this molecule also remains C–C single bond at the other molecular end, whose flexibility increases the freedom of the packing in the crystal. There is, therefore, potential interest in studying salts containing this donor combined with paramagnetic anions in the development of new organic/inorganic hybrid molecular materials. Here we report the synthe-
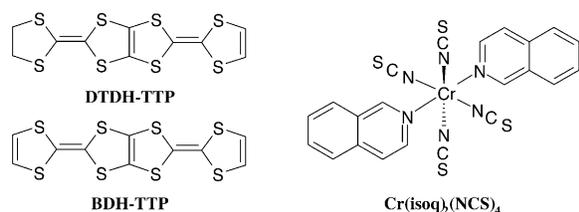
Fig. 1. Structures of DTPH–TTP, BDH–TTP and Cr(isoq)$_2$(NCS)$_4$.

sis, X-ray crystal structure and magnetic properties of (DTDH–TTP) [Cr(isoq)$_2$(NCS)$_4$] (Fig. 1).

2. Experimental

2.1. Synthesis

The solvents were distilled under nitrogen atmosphere before use and the starting reagents were used as received. Black crystals of the title compound were obtained by galvanostatic ($I = 1 \mu A$) oxidation of DTDH–TTP [12] (8 mg) under argon atmosphere, using (isoqH)[Cr(isoq)$_2$(NCS)$_4$]·3 H$_2$O [8] (100 mg) in CH$_2$Cl$_2$ (20 ml) as electrolytes.

2.2. Crystallographic data collection and structure determination

Single crystal of the title compound was mounted on a Nonius four-circle diffractometer equipped with a CCD camera and a graphite monochromated Mo Kα radiation source ($\lambda = 0.710\,73$ Å). Effective absorption correction was performed (SCALEPACK [13]). Structure was solved with direct methods and refined with full matrix least squares method on F^2 using SHELX-97 [14] programs. Crystallographic data are summarized in Table 1. Full bond lengths and bond angles, atomic coordinates and complete crystal structure results are deposited as supplementary materials.

2.3. Physical property measurements

Magnetic susceptibility was measured using a Quantum Design MPMS-5 SQUID magnetometer down to 1.8 K with an applied field of 0.1 T. Non-oriented microcrystalline sample (2.8 mg) was wrapped with an aluminium foil, whose contribution was subtracted from the observed data.

Table 1
Crystal data and structure refinement

Empirical formula	C$_{32}$H$_{20}$CrN$_6$S$_{12}$
Formula weight	925.26
Temperature (K)	293(2)
Radiation, λ/Å	Mo Ka, 0.710 73
Crystal system	Monoclinic
Space group	$C2/c$ (# 15)
a (Å)	16.0836(5)
b (Å)	19.2448(6)
c (Å)	12.6829(6)
α (°)	90
β (°)	95.669(1))
γ (°)	90
V (Å^3)	3906.5(2)
Z	4
d$_{calc}$ (g cm^{-3})	1.573
μ (mm^{-1})	0.969
Reflections collected	8792
Independent reflections	4476
[$I > 2 \sigma(I)$]	2899
Final R_1[a], wR_2[b]	0.0515, 0.1248

[a] $R_1 = \Sigma ||Fo| - |Fc||/\Sigma|Fo|$
[b] $wR_2 = \{\Sigma[w\,(Fo^2 - Fc^2)^2]/\Sigma[w(Fo^2)^2]\}^{1/2}$

3. Results and discussion

3.1. Crystal structure

Selected bond distances and bond angles are given in Table 2. ORTEP drawing [15] of the molecular structure with the atomic numbering scheme is shown in Fig. 2.

The title compound is isostructural to the previously reported salt (BDH–TTP)[Cr(isoq)$_2$(NCS)$_4$] [11]. The asymmetric unit contains half of an anion and half of a DTDH–TTP molecule, both lying on inversion centres in special positions, (1/4, 1/4, 0) and (1/4, 1/4, 1/2), respectively. The Cr–N (of NCS) distances (average value 1.988(3)Å) are slightly shorter than those to isoquinoline (Cr–N3 = 2.085(3) Å), hence the CrN$_6$ coordination octahedra is axially distorted. As the organic molecule on the inversion centre is asymmetric, it namely contains one single C–C bond in one side and a double C=C bond in the other side, and lies on the inversion centre, this unit should be orientationally disordered. However, we did not detect this disorder from the X-ray analysis. From the 1:1 stoichiometry, the charge on the donor molecule is assumed equal to +1. As shown in Fig 2b, the cations and anions form mixed zigzag layers within the bc-plane, which are

Table 2
Selected bond lengths (Å) and angles (°)

Cr–N(1)	1.988(3)	S(5)–C(14)	1.731(4)
Cr–N(2)	1.987(3)	S(5)–C(16)	1.742(6)
Cr–N(3)	2.085(3)	S(6)–C(14)	1.739(4)
S(4)–C(12)	1.729(4)	S(6)–C(15)	1.771(5)
S(4)^i–C(13)	1.749(4)	C(1)–S(1)	1.612(4)
S(3)–C(12)	1.729(4)	C(2)–S(2)	1.614(4)
S(3)–C(13)	1.736(4)	C(12)–C(12)^i	1.358(7)
C(15)–C(16)	1.379(8)		
N(1)–Cr–N(2)	90.0(1)	C(14)–S(5)–C(16)	95.5(2)
N(1)–Cr–N(3)	90.5(1)	C(14)–S(6)–C(15)	95.6(2)
N(2)–Cr–N(3)	89.6(1)	C(1)–N(1)–Cr	176.5(3)
C(12)–S(3)–C(13)	93.8(2)	C(2)–N(2)–Cr	172.2(3)
C(12)–S(4)–C(13)^i	93.4(2)		

i: $-x - 1/2, - y + 1/2, - z - 1$

then stacked along the *b*-direction. The layer consists of one-dimensional chains elongated to the *c*-direction (Fig. 3). The S···S distances of the short intermolecular contacts within the chain (S2···S3: 3.350(2), S2···S4: 3.419(2), S1···S5: 3.420(2) Å) are remarkably shorter than the van der Waals distance (3.70 Å) [16]. The adjacent chains are then connected with a π–π overlap of isoquinoline moieties (interplanar separation: $d = 3.64$ Å) between the anions, and short S···S contact (S5···S5 = 3.621(3) Å) between the donors. In the [101] direction, the neighbouring anions are related by the *c*-glide plane, and therefore the orientation of these anions is different; the angle between the molecular axes (defined as isoq–Cr–isoq axes) is 7.7(3)°. The difference in the orientation of the units in the [101] direction can be seen more clearly considering the DTDH–TTP donors that are orthogonal to each other.

3.2. Magnetic properties

Fig. 4 shows the temperature dependence of χ T and χ^{-1} measured at 0.1 T, where χ is the molar magnetic susceptibility for non-oriented microcrystalline sample after subtracting core diamagnetism contribution ($= -4.67 \times 10^{-4}$ emu mol^{-1}). The susceptibility obeys the Curie–Weiss law above ca. 50 K with the Curie constant $C = 2.35$ emu K mol^{-1} and the Weiss temperature $\Theta = -20$ K. The Curie constant is close to the corresponding spin-only value (2.25 emu K mol^{-1}) for non-interacting anion ($S = 3/2$) and donor ($S = 1/2$) spins. Below 50 K, χ T decreases as the temperature decreases, showing the antiferromagnetic coupling be-

tween the anion and donor spins. At $T_C = 8.7$ K, χ T shows a steep increase due to a magnetic transition. The inset in Fig. 4 presents the field-cooled magnetization (FCM) measured at 0.1 T, and the remanent magnetization (RM) observed after the external field of 0.1 T is removed at 1.8 K. Below $T_C = 8.7$ K, the FCM steeply increases and the RM also emerges, showing the presence of the spontaneous magnetization. When comparing the present DTDH–TTP salt with the isomorphous (BDH–TTP)[Cr(isoq)$_2$(NCS)$_4$] [11], the magnetic transition temperature is slightly increased, whereas the Weiss temperature remains in the same value. Since a one-dimensional system does not take place in a magnetic ordering in the finite temperature, the magnetic transition is realized by the inter-chain interactions and the transition temperature is governed by their strength. The S···S contacts between the donors in the adjacent chains (S5···S5: 3.621(2) Å) are slightly shorter than in the BDH–TTP salt (3.639(2)Å). This decrease of the inter-chain S···S distance between donors may be responsible to the increase of T_C in the present DTDH–TTP salt. In the same time, the HOMO of DTDH–TTP calculated using a semi-empirical PM5 Hamiltonian [17] (Fig. 5) is more delocalised to the outer sulphur atoms (S5 and S6 in Fig. 2a) compared to BDH–TTP due to the presence of the terminal C=C double bond. As a result, inter-chain exchange interactions between donors are increased, which also works to elevate T_C of this compound.

Fig. 6 shows the magnetization curves at $T = 2$ K measured on non-oriented crystalline samples. As the field increases, the magnetization tends to reach the

a

b
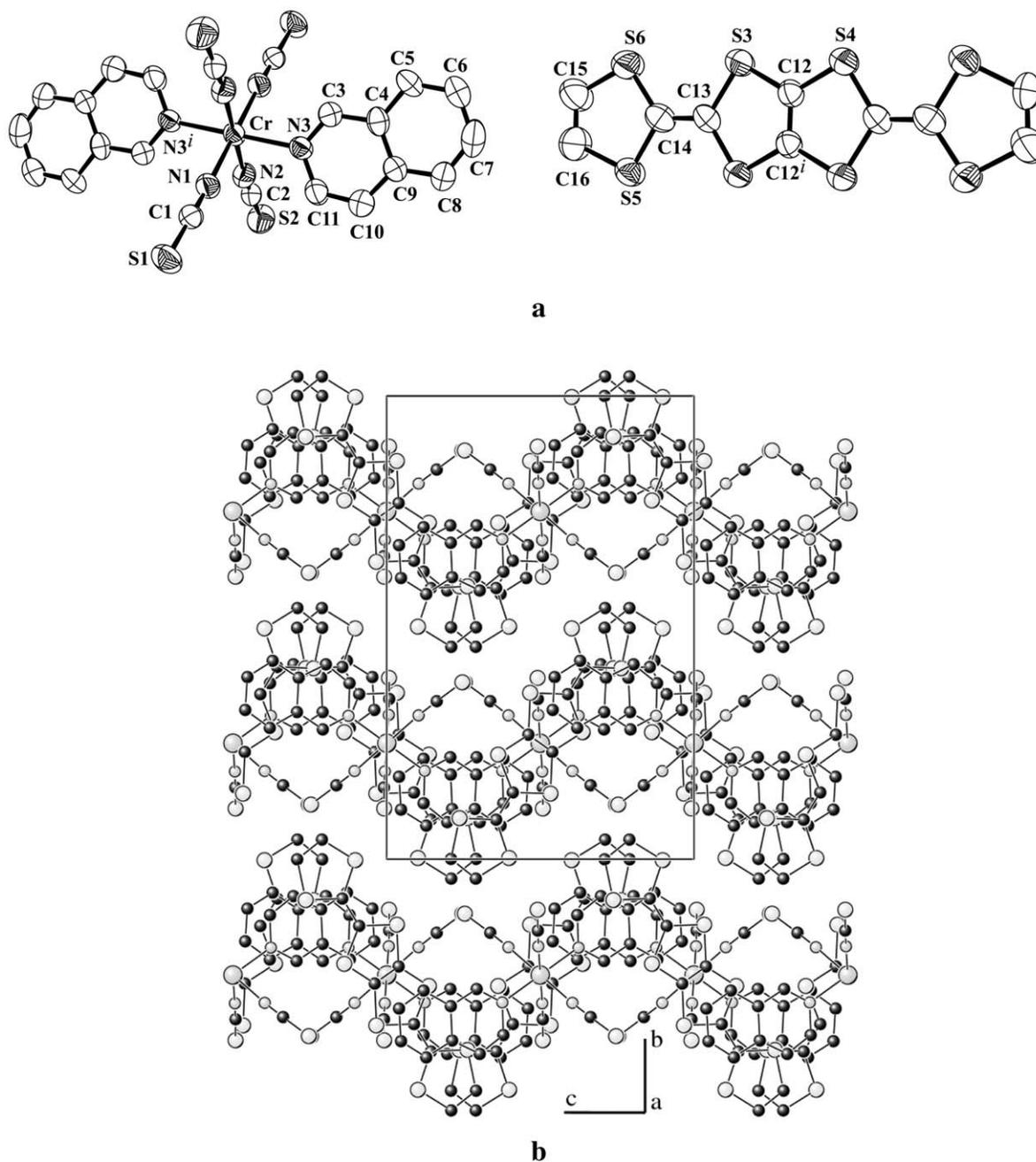
Fig 2. (**a**) ORTEP diagram with 50% probability level and atom numbering scheme; (**b**) projection of the crystal structure onto the *bc* plane, showing the π overlap between the isoquinoline ligands and the DTDH–TTP molecules.

value of $2\,\mu_B$, showing that all anion spins ($S = 3/2$) and donor spins ($S = 1/2$) are aligned anti-parallel to form ferrimagnetic chains. On the magnetization curve, a broad anomaly is observed at $B = 1$ T, which is more clearly shown as a peak in the dM/dB vs. B plot (lower panel of Fig. 6). From the analogy to the previous result on the BDH–TTP salt [11], this anomaly should be assigned to a spin-flop transition. Around $B = 0$ T, a
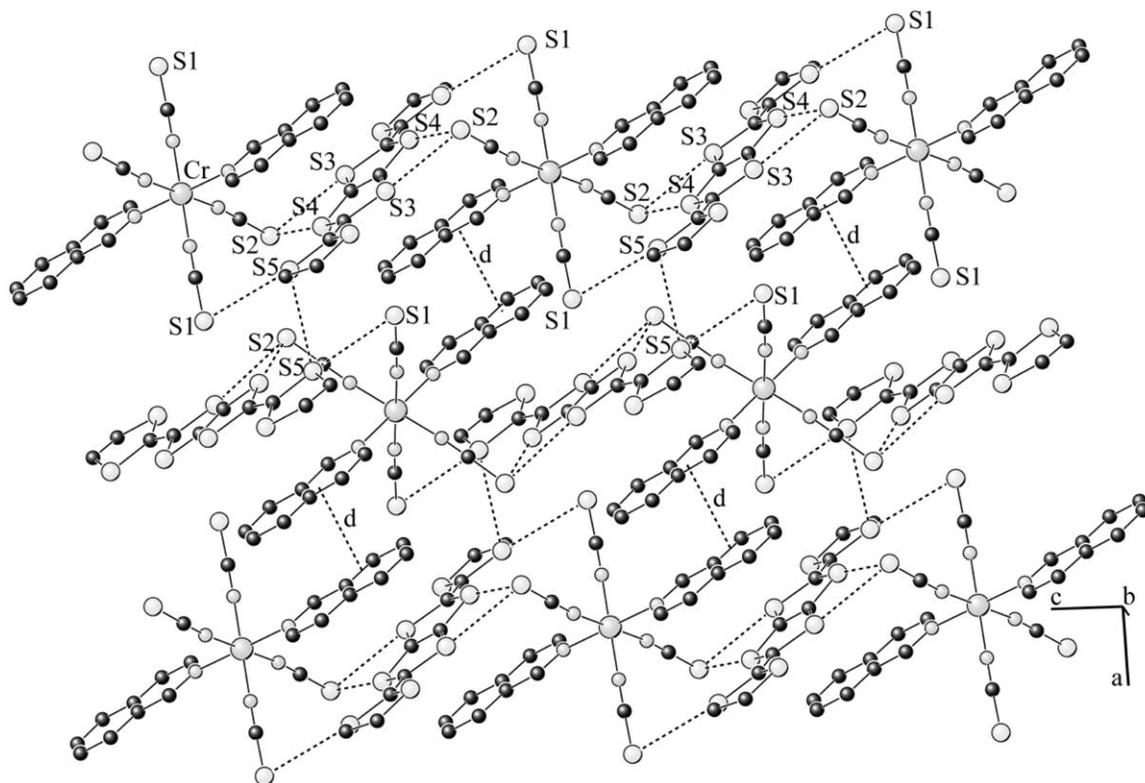
Fig. 3. Projection of the mixed layer onto the *ac* plane showing the mixed chain of anion and donor; dotted lines indicate the anion–anion overlap (interplanar separation: d = 3.64 Å) and intermolecular S···S contacts (S2···S3: 3.350(2), S2···S4: 3.419(2), S1···S5: 3.420(2), S5···S5: 3.621(2) Å).
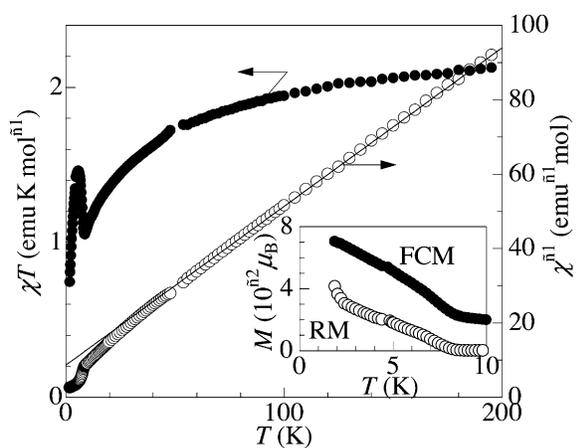
Fig. 4. Temperature dependence of χT (filled circles) and χ^{-1} (open circles), where χ is the molar paramagnetic susceptibility. Solid line is the Curie–Weiss fitting (C = 2.25 emu K mol^{-1}, Θ = –20 K). Inset: temperature dependence of the field-cooled (•) and remanent magnetization (○).

DTDH–TTP
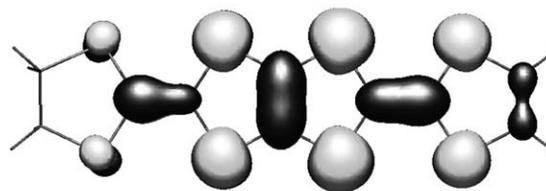
BDH–TTP
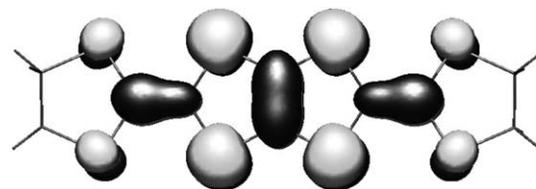
Fig. 5. The HOMOs of DTDH–TTP (top) and BDH–TTP (bottom), calculated using a semi-empirical method using PM5 Hamiltonian.
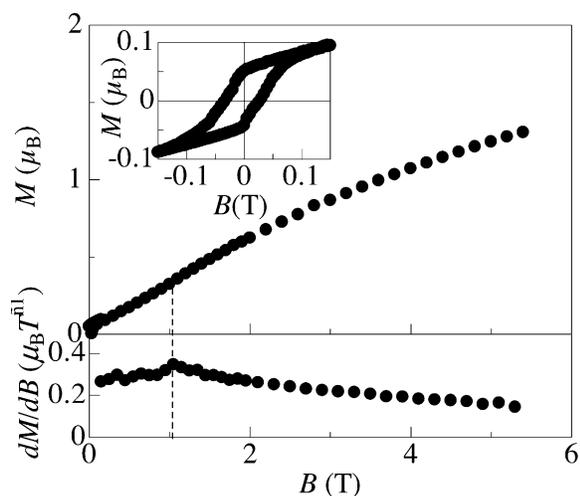
Fig. 6. Field dependence of the magnetization M (top) and dM/dB (bottom) measured at 2 K. Insets: hysteresis loop around $B = 0$ T.

hysteresis loop is observed, which is consistent with the presence of the remanent magnetization. Although the present magnetic data are based on the non-oriented sample, it is reasonable to assume that the spontaneous magnetization is parallel to the b-axis direction (perpendicular to the two-dimensional sheets of the donors and anions), since this salt is isostructural to (BDH–TTP)[Cr(isoq)$_2$(NCS)$_4$] whose magnetic structure has been clarified from the single-crystalline data. From this hysteresis loop, we can estimate the remanent magnetization along the b-axis from the hysteresis loop at $0.05/\overline{\cos\theta} = 0.10\ \mu_B$, where $\overline{\cos\theta} = 1/2$ is the average value of the direction cosine. The spin-canting angle is therefore estimated at $\sin^{-1}(0.10\ \mu_B/2\ \mu_B) = 2.9°$, which is same as the corresponding value of (BDH–TTP)[Cr(isoq)$_2$(NCS)$_4$]. This accordance in the canting angle for both compounds is reasonable, since the spin canting is derived from the single-ion anisotropy caused by the uniaxial distortion of CrN$_6$ coordination octahedron and canting of these anisotropy axes, similarly in both BDH–TTP and DTDH–TTP salts.

4. Conclusion

A new molecular weak ferromagnet was prepared and characterized. This compound contains mixed chains of anions and radical cations that give rise to a ferromagnetic spin structure. These ferrimagnetic chains interact antiferromagnetically with each other through $\pi\cdots\pi$ overlap between isoquinoline ligands of neighbouring anions and S$\cdots$S contacts between donor molecules, but since these chains are not related by lattice translation, a canting angle is observed between them leading to a weak canted ferromagnetic long-range ordering. The title compound (DHDT–TTP) [Cr(isoq)$_2$(NCS)$_4$] is isostructural to BDH–TTP salt with the same anion but show higher T_C (8.7 K instead of 7.6 K).

5. Supplementary Material

The supplementary material has been sent to the Cambridge Crystallographic Data Centre, 12 Union Road, Cambridge CB2 1EZ, UK, as supplementary material CCDC 195693 and can be obtained by contacting the CCDC (quoting the article details and the corresponding SUP number).

References

[1] A.W. Graham, M. Kurmoo, P. Day, J. Chem. Soc, Chem. Commun. (1995) 2061.

[2] H. Kobayashi, A. Kobayashi, P. Cassoux, Chem. Soc. Rev. 29 (2000) 325 and references cited therein.

[3] P. Le Maguerès, L. Ouahab, N. Conan, C.J. Gomez-García, P. Delhaès, J. Even, M. Bertault, Solid-State Commun. 97 (1) (1996) 27.

[4] J. Nishijo, A. Miyazaki, T. Enoki, E. Ogura, T. Takano, Y. Kuwatani, M. Iyoda, J. Yamaura, Solid-State Commun. 116 (2000) 661.

[5] D. Thoyon, K. Okabe, T. Imakubo, S. Golhen, A. Miyazaki, T. Enoki, L. Ouahab, Mol. Cryst. Liq. Cryst. 376 (2002) 25.

[6] L. Ouahab, Chem. Mater. 9 (1997) 1909.

[7] E. Coronado, J.R. Galan-Mascaros, C.J. Gomez-García, V.N. Laukhin, Nature 408 (2000) 447.

[8]   S.S. Turner, C. Michaut, S. Durot, P. Day, T. Gelbrich, M.B. Hursthouse, J. Chem. Soc., Dalton Trans. (2000) 905.

[9]   F. Iwahori, S. Golhen, L. Ouahab, R. Carlier, J.-P. Sutter, Inorg. Chem. 40 (2001) 6541.

[10] J. Yamada, T. Toita, H. Akutsu, S.-I. Nakatsuji, H. Nishikawa, I. Ikemoto, K. Kikuchi, Chem. Commun. (2001) 2538.

[11] F. Setifi, L. Ouahab, S. Golhen, A. Miyazaki, K. Okabe, T. Enoki, T. Toita, J. Yamada, Inorg. Chem. 41 (2002) 3786.

[12] J. Yamada, S. Mishima, H. Anzai, M. Tamura, Y. Nishio, K. Kajita, T. Sato, H. Nishikawa, I. Ikemoto, K. Kikuchi, J. Chem. Soc., Chem. Commun. (1996) 2517.

[13] Z. Otwinowski, W. Minor, Processing of X-ray Diffraction Data Collected in Oscillation Mode, in: C.W. Carter Jr, R.M. Sweet (Eds.), Macromolecular Crystallography, Part A, Methods Enzymol 276 (1997) 307.

[14] G.M. Sheldrick, SHELX 97, Program for the Refinement of Crystal Structures, University of Göttingen, Germany, 1997.

[15] M.N. Burnett, C.K. Johnson, ORTEP–III: Oak Ridge Thermal Ellipsoid Plot Program for Crystal Structure Illustrations Oak Ridge National Laboratory Report ORNL–6895, 1996.

[16] A. Bondi, J. Phys. Chem. 68 (1964) 441.

[17] J.J.P. Stewart, 'MOPAC 2002', Fujitsu Limited, Tokyo, Japan, 2001.